

# Vertical flux and fate of particulate matter in a Newfoundland fjord at sub-zero water temperatures during spring

R. J. Thompson<sup>1</sup>, D. Deibel<sup>1,\*</sup>, A. M. Redden<sup>2</sup>, C. H. McKenzie<sup>3</sup>

<sup>1</sup>Ocean Sciences Centre, Memorial University, St. John's, Newfoundland and Labrador A1C 5S7, Canada

<sup>2</sup>Acadia Centre for Estuarine Research, Acadia University, Wolfville, Nova Scotia B4P 2R6, Canada

<sup>3</sup>Northwest Atlantic Fisheries Centre, Department of Fisheries and Oceans Canada, St. John's, Newfoundland and Labrador A1C 5X1, Canada

**ABSTRACT:** To test the hypothesis that low temperature inhibits utilization of sinking spring bloom material, we studied the formation and fate of the bloom in Conception Bay, Newfoundland, Canada, where the entire water column is  $<0^{\circ}\text{C}$  during the spring bloom and the benthos is  $<-1^{\circ}\text{C}$  year round. The bloom formed in April and sank from the upper mixed layer in May, following nutrient depletion in the upper 50 m. Using sediment traps (40, 80, 150, and 240 m depth), we determined time-averaged fluxes of total particulate matter, particulate organic carbon, particulate organic nitrogen, and chlorophyll *a* as the material sank to the bottom. The sinking material was dominated by zooplankton fecal pellets before and after the sinking event, but by diatom vegetative cells and spores during it. Over half (56%) of the primary production during the spring bloom was exported from the upper mixed layer. The principal fate of sinking phytodetritus was aerobic utilization by benthic microorganisms (42%), followed by consumption by water column zooplankton (18%). Although rates of primary production and sinking in Conception Bay were not exceptional in a global context, the quality of the sinking material was extremely high in terms of properties such as percent organic matter, percent carbon, and percent nitrogen. We found little evidence for low temperature regulation of the utilization of organic carbon from the spring bloom in Conception Bay, but we propose a role of low temperature in maintaining high nutritional quality of sinking phytodetritus.

**KEY WORDS:** Vertical flux · Sediment trap · Spring bloom · Pigments · Temperature · Benthos

—Resale or republication not permitted without written consent of the publisher—

## INTRODUCTION

The sedimentation of spring phytoplankton is a common feature of temperate and polar coastal seas (Beaulieu 2002, Tian et al. 2003, Tamelander & Heiskanen 2004). Although fecal pellets produced by herbivorous zooplankton are generally important in the vertical flux of phylogenous material (Bathmann et al. 1987), sedimentation of ungrazed phytoplankton during spring blooms is often quantitatively more important than fecal pellet flux (Smetacek 1985a, Andreassen & Wassmann 1998), perhaps due to a relatively low biomass of overwintering herbivorous zooplankton, particularly in cold, northern waters (Smetacek

1985b, Ramos et al. 2003). Furthermore, a temporal lag in the numerical response of zooplankton populations to a short period of rapid phytoplankton growth may result in limited grazing impact during spring (Dagg et al. 1982, Parsons 1988). Consequently, a large portion of the phytoplankton biomass settles out of the euphotic zone in the form of intact cells, cysts, diatom chains, and flocs during the senescent stage of the bloom (Smetacek 1985a, Ramos et al. 2003, Tamelander & Heiskanen 2004).

Sedimentation during spring blooms supplies significant amounts of organic matter and energy to suprabenthic, epibenthic, and benthic environments, directly linking phytoplankton production to food

\*Corresponding author. Email: ddeibel@mun.ca

webs beneath the euphotic zone (Fabiano et al. 2001, Beaulieu 2002, Mincks et al. 2005). The spring pulse of sinking organic matter is often the principal energy source for these communities. In temperate and high latitudes, as much as half of the annual input of organic matter to the benthos is deposited during spring (Townsend & Cammen 1988, Grebmeier & McRoy 1989). The response to sinking phytodetritus is often rapid throughout the food web, from bacteria and protists to benthopelagic peracarid crustaceans and benthic bivalves (Pomeroy et al. 1991, Drazen et al. 1998, Glud et al. 1998, Stead & Thompson 2003, Richoux et al. 2004a,b), although other studies have reported little response of the benthos to pulses of phytodetritus (Josefson et al. 2002, Mincks et al. 2005). In bays and fjords of temperate regions, zooplankton grazing may play an important role in the transport of organic carbon and may be the primary contributor to the vertical flux of phytoplankton production (Peinert et al. 1989, Juul-Pedersen et al. 2006).

Although Newfoundland fjords are located in mid-latitudes, their oceanographic characteristics are typical of sub-arctic seas, owing to the influence of the Labrador Current (de Young & Sanderson 1995). Given these conditions, which of the following patterns for utilization of the spring bloom should we expect in a Newfoundland fjord: close coupling, with high rates of bacterial and zooplankton utilization of sinking material in the water column, or weak coupling, resulting in high rates of organic matter flux to the benthos?

Conception Bay is located on the east coast of the island of Newfoundland, Canada, and is oriented roughly northeast to southwest, opening onto the inshore branch of the Labrador Current (Fig. 1). The fjord is approximately 25 km wide  $\times$  85 km long, with a maximum depth in the southwestern depositional basin of about 300 m and a sill at 150 m. Pack ice may occur from mid-March to late April, depending on the concentration of ice offshore and the frequency and duration of onshore, northeasterly winds. Freshwater runoff is relatively insignificant within the bay compared to sea-ice melt upstream. Water temperatures are generally low in Conception Bay, which has a permanent cold intermediate layer (80 to 120 m depth) that remains  $<0^{\circ}\text{C}$  year round and a near-bottom water mass that never exceeds  $-0.8^{\circ}\text{C}$  (Pomeroy et al. 1991, deYoung & Sanderson 1995), a fact that has been overlooked in the literature (e.g. Rysgaard et al. 1998). These low temperatures may have a profound effect on heterotrophic utilization of the products of primary production in the water column, both by bacteria (Pomeroy et al. 1991, Budge & Parrish 2003, Mincks et al. 2005) and by zooplankton (Parsons 1988). However, Pomeroy et al. (1991) reported relatively high rates of carbon remineralization in the surficial sediments of

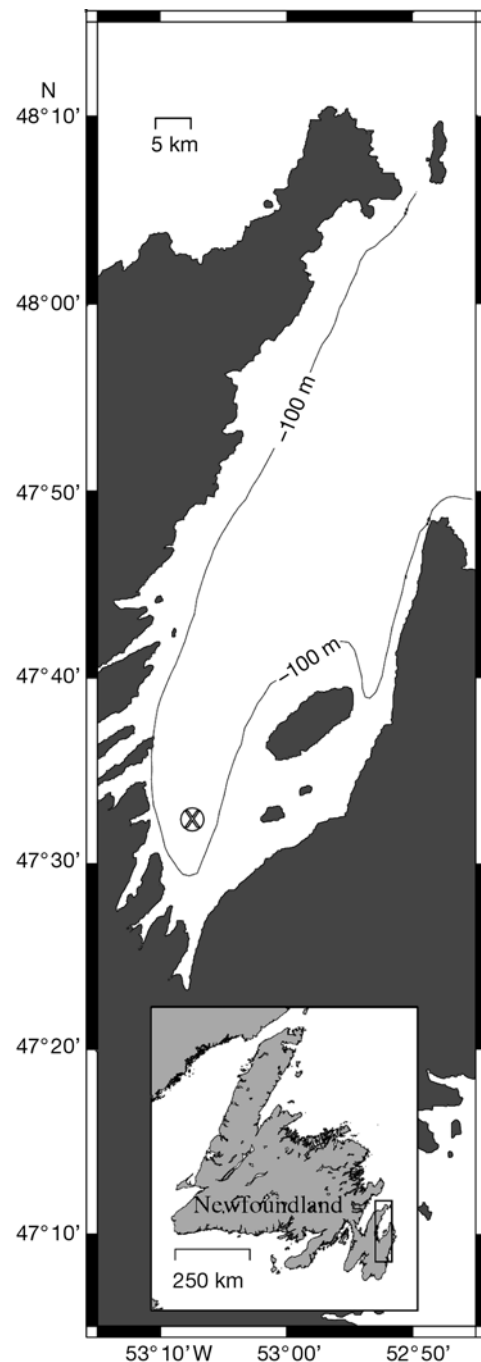


Fig. 1. Site of the sediment trap mooring in Conception Bay, Newfoundland (depth 270 m)

Conception Bay despite the low temperature, consistent with subsequent reports of high rates of organic carbon utilization in Arctic fjords and Antarctic shelf waters (Glud et al. 1998, Baldwin & Smith 2003, Mincks et al. 2005). Because of the mid-latitude light regime, we hypothesized that the diatom bloom in Conception Bay should begin before the onset of thermal stratification and therefore at very low water tem-

peratures, leading to suppression of bacterial and mesozooplankton utilization of phytoplankton production in the water column and to high flux of diatom biomass to the bottom. Conversely, in those years when meteorological and hydrographic factors either delay or prolong the spring bloom, utilization of phytodetritus by water column heterotrophs should be greater (Townsend et al. 1994). According to Rysgaard et al. (1998), much of the literature on benthic-pelagic coupling concerns warm, shallow water with a seasonal cycle in bottom water temperature (Olesen 1995, Heiskanen & Leppänen 1995), complicating interpretation of heterotrophic response data. In contrast, water temperature below 80 m depth varies little in Conception Bay throughout the year, and the entire water column remains  $<0^{\circ}\text{C}$  throughout the formation and sinking of the spring phytoplankton bloom (Parrish et al. 2005). In this study, we determined the vertical flux of particulate matter in order to estimate the input of energy to the benthos of Conception Bay during spring and to test our hypotheses concerning pelagic utilization of the bloom. This work was conducted as part of the Cold Ocean Productivity Experiment (COPE), an international research program to investigate heterotrophic utilization of the spring bloom at low water temperatures. Although there is considerable information from temperate and tropical waters, pelagic-benthic energy coupling is poorly documented in sub-arctic regions, largely because of strong seasonal variation in climatic forcing and primary production as well as an incomplete understanding of food web structure and dynamics (Beaulieu 2002, Hobson et al. 2002, Wassmann et al. 2004).

## MATERIALS AND METHODS

**Vertical flux.** The vertical flux of particulate material was determined with sediment traps moored at a site within the deep depositional area of Conception Bay, before, during, and after the spring phytoplankton bloom in 1988 (Fig. 1). A series of traps was attached to a taut-wire mooring at a site 270 m deep (Fig. 1). The traps were  $60 \times 10$  cm PVC cylinders (Bloesch & Burns 1980), giving a collection efficiency equivalent to that of funnel traps with baffles (Hargrave & Burns 1979). Arrays of 4 replicate traps equally spaced on the circumference of a circle with a diameter of 1 m were deployed at each of 4 depths (40, 80, 150, and 240 m below

the surface) for periods of 3 to 7 d, with one 13 d deployment during early April due to a prolonged storm (Table 1). Traps were retrieved 10 times between 29 March and 30 May. At each retrieval, and on other sampling dates when traps were not retrieved, vertical profiles of water column properties were recorded (SeaBird SBE 25 CTD fitted with a SeaTech *in situ* fluorometer). CTD data were smoothed into 2 m bins before contour plotting. Relative fluorescence units were converted to chlorophyll (chl) *a* concentrations using a regression equation based on samples from Conception Bay (Ostrom et al. 1997).

During the first 5 trap deployments, 2 traps of each quartet at 40, 80, and 150 m were covered with plastic screens (1.8 mm mesh) to exclude ‘swimmers’ while permitting diatom chains, flocs, and fecal pellets to enter. No significant differences ( $p > 0.05$ ) were obtained in the mean value for any variable between traps with screens and those without (data not shown), so the practice of using screens was discontinued in later deployments, and data from traps with and without screens were pooled before statistical analyses and plotting. Poisons were not used, as the duration of deployment was short, and water temperatures were low. Furthermore, poisons interfere with the chemical analyses of samples, e.g. by partial destruction of chl *a* (Olesen 1995), and increase the number of swimmers retained (Olesen 1995, Parrish et al. 2005). Other studies in this region suggest that omitting poisons results in a loss of  $<10\%$  of particulate organic carbon (POC) and greatly reduces variability due to the elimination of zooplankton swimmers (Parrish et al. 2005). Recent publications have recommended non-poisoned

Table 1. Trap deployment information. Traps were deployed in quadruplicate on a taut-wire train wheel mooring at 4 depths (40, 80, 150, and 240 m below surface) in Conception Bay, Newfoundland. The maximum temperature shown is the mean temperature at the near surface (40 m) trap during each deployment as determined with a Seabird SBE-25 CTD (see ‘Materials and methods’). The maximum temperatures recorded at all other trap depths were less than this near-surface value. The letter code for the various deployments (A–J) is for cross-reference to Figs. 2 to 5

Sequential deployment number	Maximum temperature ( $^{\circ}\text{C}$ )	Date trap deployed	Date trap retrieved	Elapsed time of deployment (d)	Deployment code
01	-1.03	29 March	6 April	8	A
02	-0.32	6 April	19 April	13	B
03	-0.33	19 April	22 April	3	C
04	-0.91	22 April	27 April	5	D
05	-0.66	27 April	4 May	7	E
06	0.19	4 May	10 May	6	F
07	0.64	10 May	13 May	3	G
08	-0.56	13 May	17 May	4	H
09	-0.14	17 May	25 May	8	I
10	-0.77	25 May	30 May	5	J

traps for flux studies in cold water (Tamelander & Heiskanen 2004, Wassmann et al. 2004).

One hour after trap recovery, the bulk of the supernatant from each collection tube was slowly decanted and discarded, taking care not to disturb the settled material. The remaining supernatant and contents were returned to the laboratory in polycarbonate bottles packed in ice. Zooplankton were removed from the samples, which were then allowed to settle overnight on ice. The supernatant was again carefully decanted, as described above, and the remaining slurry made up to 50 or 100 ml with filtered seawater (1  $\mu\text{m}$  in-line cartridge filter). The slurry was thoroughly mixed by gentle shaking, and subsamples were removed for analysis.

Ideally, flux measurements based on sediment trap data should be made in environments with low current velocities, to avoid resuspension of benthic material and hydrodynamic interactions between turbulent flow fields and the mouth of the trap, and to minimize small horizontal gradients in the concentration of sinking particles. Mean current velocities at 25 m depth near the trap mooring in Conception Bay in spring and summer are low ( $<2\text{ cm s}^{-1}$ ) and cause negligible net horizontal transport (deYoung & Sanderson 1995). Tidal currents do not play a major role in water mass exchange or in the mean circulation in Conception Bay, and the residence time of surface water near the trap mooring is about 30 d (deYoung & Sanderson 1995). Near the western shore of the bay, to the west of the trap mooring, currents are weak, variable, and oriented parallel to the isobaths, suggesting that advection from coastal waters into the deep depositional area is unlikely. The mean circulation pattern is generally cyclonic (deYoung & Sanderson 1995), suggesting that to the east of the trap mooring current flow is directed away from the study site (Fig. 1). Current velocities at 200 m are generally lower than at the surface (i.e. mean velocities are  $<2.3\text{ cm s}^{-1}$ , deYoung & Sanderson 1995) and well below the threshold of  $15\text{ cm s}^{-1}$  above which the efficiency of sediment traps declines rapidly (Baker et al. 1988). Several years of transmissometer data indicate that the nepheloid layer extends to ca. 70 m above bottom (authors' unpubl. data). In those years in which multiple sediment trap moorings were deployed in Conception Bay, there was strong coherence between the inner and outer bay in both the timing and magnitude of vertical flux events (Ostrom et al. 1997). Thus data collected at our mooring site is generally representative of the timing and magnitude of vertical flux throughout the bay.

**Particulate organic carbon, particulate organic nitrogen (PON), and pigments.** For the determination of POC and PON, subsamples of trap material were collected under vacuum on pre-combusted Whatman

GF/C filters (25 mm diameter), dried at  $60^\circ\text{C}$ , and combusted in a Perkin-Elmer 240 CHN analyzer. No correction was made for carbonates, as microscopy of trap contents revealed few shell-bearing organisms and previous checks had indicated that carbonates represented  $<10\%$  of total particulate carbon. The same filtration process was used for the determination of dry weight of particulate matter and weight loss on ignition at  $450^\circ\text{C}$ , except that material on the filter was washed with 2 ml of 3% ammonium formate before drying.

Water samples for chloropigment determination were collected on 25 mm Whatman GF/C filters under low vacuum and analyzed immediately or following storage in darkness at  $-70^\circ\text{C}$  for up to 6 wk (Redden et al. 1993). Pigments were extracted overnight in 90% acetone at  $4^\circ\text{C}$  in darkness. Chl *a* and phaeopigments were determined by fluorometry, and 1 sample from each set of 4 replicates was also analyzed by HPLC (Redden et al. 1993) to check for systematic errors in fluorometric results due to interference from chl *b*, from breakdown products of chloropigments often found in zooplankton feces, or from other nonchlorophyllous, fluorescent material. Redden et al. (1993) found very good agreement between fluorescence and HPLC methods for chl *a*-like pigments and phaeopigments extracted from algal cultures and mussel feces, with no elevation of the baseline in the HPLC profiles. For routine work we therefore measured chl *a* and total phaeopigments with a Turner-Designs TD-10 fluorometer.

**Microscopic analysis.** For microscopic analysis, a 1 ml subsample was removed from the sediment trap slurry and placed in a 20 ml vial. One ml basic Lugol's iodine was added and the vial filled with the clear supernatant from the slurry bottle. After mixing, 1 ml of fixed sample was removed and placed in an Utermöhl chamber. For phytoplankton and fecal pellet identification and enumeration, up to one-half of the resulting settled material was examined at  $400\times$  and  $200\times$  magnification with a Zeiss Axiovert 35 inverted microscope under phase-contrast illumination. At least 300 cells in each taxon or size class were counted. Phytoplankton and fecal pellet volume estimates were made with an ocular micrometer by approximation to common geometric shapes. Observed phytoplankton volume was corrected for cell shrinkage due to dehydration. Many of the fecal pellets were in various stages of disintegration, making volume estimation difficult. Phytoplankton (except diatoms) and fecal pellet volume were converted to carbon using the equation  $C\text{ (pg)} = \text{volume } (\mu\text{m}^3) \times 0.11$ , while diatom volume was converted using  $C\text{ (pg)} = \text{plasma volume } (\mu\text{m}^3) \times 0.11$  (Strathmann 1967, Booth 1993). Taxonomic composition values for trap samples are expressed in this paper as relative percentages based on carbon mass, i.e.

(mass of taxon or group / total mass of recognizable particles)  $\times 100\%$ .

Water column samples for microscopic analysis were taken with 5 l Niskin bottles. Subsamples (250 ml) were fixed with basic Lugol's iodine (final concentration ca. 1%) and stored in the dark at 5°C. Further subsamples (2 to 100 ml, depending on cell abundance) were settled in Utermöhl chambers. Floristic analysis followed the Utermöhl method as detailed for the sediment trap samples above.

**Inorganic nutrients.** Additional water samples were removed from the Niskin bottles and stored in the dark on ice until inorganic nutrient analyses were completed, within 24 h of collection (Strickland & Parsons 1972). Reactive silicate was determined by the molybdate method and nitrate by the sulfanilamide reaction.

**First-order seasonal carbon budget.** A first-order carbon budget for the 79 d period covering the formation and sinking of the spring phytoplankton bloom was constructed using a combination of data from Conception and Trinity Bays, Newfoundland, reported in this paper and previous publications outlined below. Here we present the sources of data and assumptions underlying the carbon budget.

The seasonal primary production rate of 45 gC m<sup>-2</sup> was taken from this paper, in which the sources and assumptions are given. Daily utilization of organic carbon by bacteria in the water column was taken from bacterial biomass and production data for Conception Bay (Pomeroy et al. 1991), assuming a bacterial growth efficiency of 33%, which is in the mid-range of values reported by these authors. Daily rates were temporally integrated by rectangular interpolation. Utilization of organic carbon by water column mesozooplankton was based on zooplankton biomass information for Conception Bay (Tian et al. 2003), assuming a mesozooplankton daily ration of 30% of body carbon from copepod ingestion rate data for Conception Bay (Redden 1994), and an assimilation ratio of 70% derived from a synthesis of literature on copepods and appendicularian tunicates. The zooplankton biomass value used was 0.5 gC m<sup>-2</sup> (note error in units in the original figure of Tian et al. 2003), which is a conservative estimate for Conception Bay (see Discussion). Daily zooplankton carbon utilization was multiplied by 79 d to cover the entire sinking period. The estimated benthic flux of organic carbon was derived from the sediment trap data presented here.

Utilization of organic carbon by anaerobic benthic microbes was taken from data for Conception Bay sediments (Pomeroy et al. 1991), assuming a bacterial growth efficiency of 33%, the mid-range of values recommended by Pomeroy et al. (1991). Aerobic benthic microbial utilization of organic carbon was estimated assuming a benthic respiration rate of 107 mgC m<sup>-2</sup> d<sup>-1</sup>

and a bacterial growth efficiency of 33%, both from Conception Bay sediment data (Pomeroy et al. 1991). The result was a benthic microbial utilization rate of 162 mgC m<sup>-2</sup> d<sup>-1</sup>, or 19 gC m<sup>-2</sup> for the 79 d sinking period, assuming a constant proportion of benthic aerobic utilization of the sinking material over the entire sinking period (G. T. Rowe pers. comm.).

Utilization of organic carbon by suprabenthic zooplankton was estimated assuming an abundance of 200 *Pseudocalanus* spp. m<sup>-2</sup> (primarily copepodite stage IV with a mass of 3.5 µgC animal<sup>-1</sup>) and 25 *Calanus* spp. m<sup>-2</sup>, most of which were copepodite stage IV with a mean mass of 50 µgC animal<sup>-1</sup> (Choe & Deibel 2000). A daily ration of 30% was assumed for suprabenthic copepods, as for water column copepods (see above). Daily carbon utilization rates were multiplied by 79 d. Mysids are also abundant in the benthic boundary layer, and their utilization of organic carbon was calculated from abundance and biomass data from sledge tows in Conception Bay (Richoux et al. 2004c). We assumed a daily ration of 30% of body weight for mysids and an assimilation ratio of 70%. Daily carbon utilization rates were multiplied by 79 d. The carbon utilization by suprabenthic zooplankton was the sum of the above rates for suprabenthic copepods and mysids.

Utilization of organic carbon by macrobenthos was based upon a macrobenthic biomass of 5 gC m<sup>-2</sup> for Conception Bay (Scheibe 1991), and a daily ration of 1% and assimilation ratio of 70% for Conception Bay macrobenthos (Stead et al. 2003). Daily rates of carbon utilization were multiplied by 79 d.

## RESULTS

### Water column properties

The first sustained doubling of winter chl *a* values was established at ca. 15 m depth on 23 to 24 March, marking the initiation of the spring bloom. There was no thermal stratification at this time, with temperatures <0°C from surface to bottom (Fig. 2a). However, there was a density difference of 0.3 between the surface and 70 m depth (Fig. 2b) because the surface water was less saline. Silicate values in the upper mixed layer (UML) were ca. 40% lower in late March than in winter (Fig. 2e). A strong and sustained storm during the first 2 wk of April terminated the nascent bloom (Fig. 2a–c). Following relaxation of the wind stress, the peak magnitude of chl *a* reached ca. 2.5 µg l<sup>-1</sup> at 30 m depth on 2 to 3 May. Surface heating contributed to increasing stratification during the first 3 wk of May (Fig. 2a,b), accompanied by a reduction of surface silicate from 4.0 to <0.5 µM and a deepening of the sub-



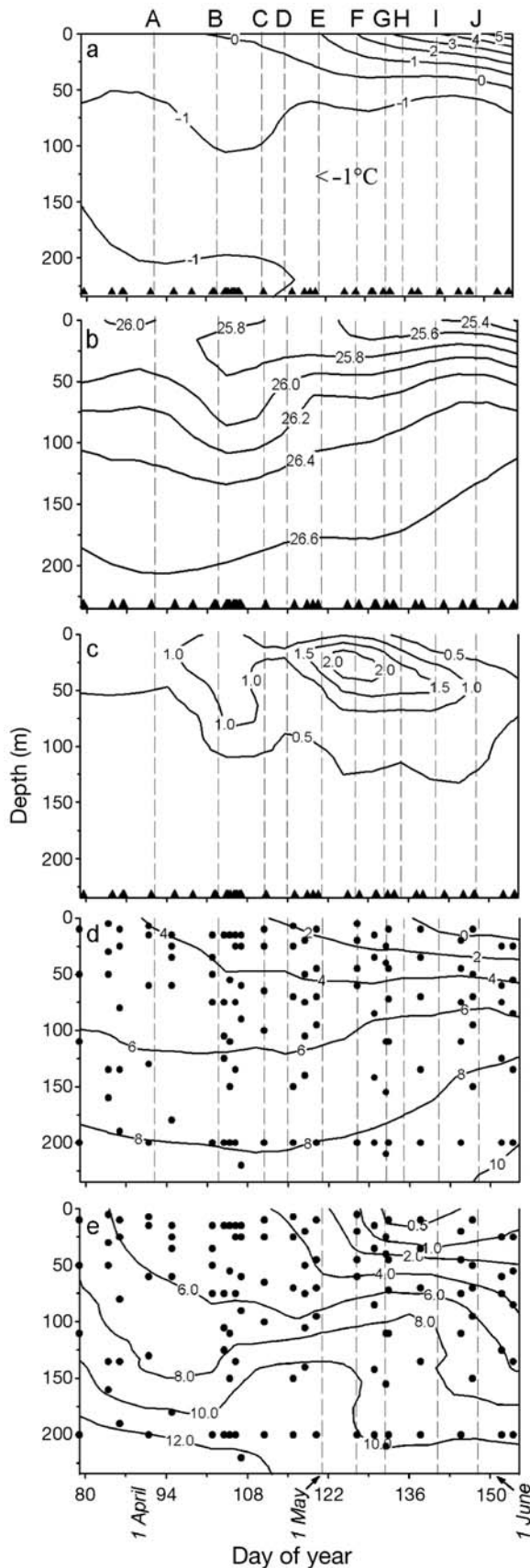


Fig. 2. Time-depth plots of hydrographic and inorganic nutrient data during the sediment trap deployments in Conception Bay. A to J and vertical dotted lines mark the retrieval of trap samples (details in Table 1). (a) Temperature ( $^{\circ}\text{C}$ ), (b) density ( $\sigma\text{-t}$ ), (c) *in situ* chl *a* ( $\mu\text{g l}^{-1}$ ). See 'Materials and methods' for the conversion of relative fluorescence units to units of chl *a*. Black triangles on the x-axes of (a–c) indicate time of CTD casts. (d) Nitrate ( $\mu\text{M}$ ), (e) silicate ( $\mu\text{M}$ ). Filled circles in (d) and (e) indicate the depths at which water samples were taken with Niskin bottles

surface chlorophyll maximum (SCM) from 30 to  $>50$  m depth (Fig. 2c). There was evidence of higher concentrations of chl *a* in the deep water mass from the last week in April through the first half of May. The SCM fell below  $0.8 \mu\text{g chl a l}^{-1}$  on 27 May, about 2 mo after the bloom began (Fig. 2c). During sinking of the bloom, the SCM was never located in water  $>0^{\circ}\text{C}$  (Fig. 2a,c).

The storm in early April greatly modified the composition of the phytoplankton community. Biomass of the pre-bloom community was dominated by unarmored dinoflagellates and ciliates. At the beginning of the bloom in late March, diatoms increased in abundance relative to flagellates in the upper 25 m. The diatom community was dominated primarily by *Chaetoceros debilis*, with a secondary contribution from *Skeletonema costatum*. The storm resulted in the reestablishment of a pre-bloom, flagellate-dominated phytoplankton community. Following the storm, diatoms once again increased in numbers relative to flagellates, with diatom biomass accounting for 90% of total community carbon by the end of April. This was followed in May by accelerated sinking of diatoms and a relative increase in dinoflagellates in the UML, with dinoflagellate biomass reaching  $>90\%$  of total community carbon by the end of May. Although *C. debilis*, *C. socialis* and *S. costatum* were the most abundant diatoms during the spring bloom period, *Thalassiosira nordenskioldii*, *T. gravida*, *T. subtilis*, and *Coscinodiscus* spp. dominated carbon mass, often making up 40 to 60% of total diatom biomass. *Thalassiosira* spp. and *Coscinodiscus* spp. dominated biomass at depths below 25 m during the second half of the bloom period.

### Particle flux

At depths of 40, 80, and 150 m, daily fluxes of total particulate matter (TPM) were 1 to  $3 \text{ g m}^{-2} \text{ d}^{-1}$  throughout April (samples A to E), increasing to  $>4 \text{ g m}^{-2} \text{ d}^{-1}$  in samples F and G in early May (Fig. 3). Organic content of the trap material at 40 and 80 m was 15–28% during April and 30–52% in May, the highest levels occurring from 4 to 10 May (sample F). During the second half of May, the sinking SCM had reached depths  $>40$  m

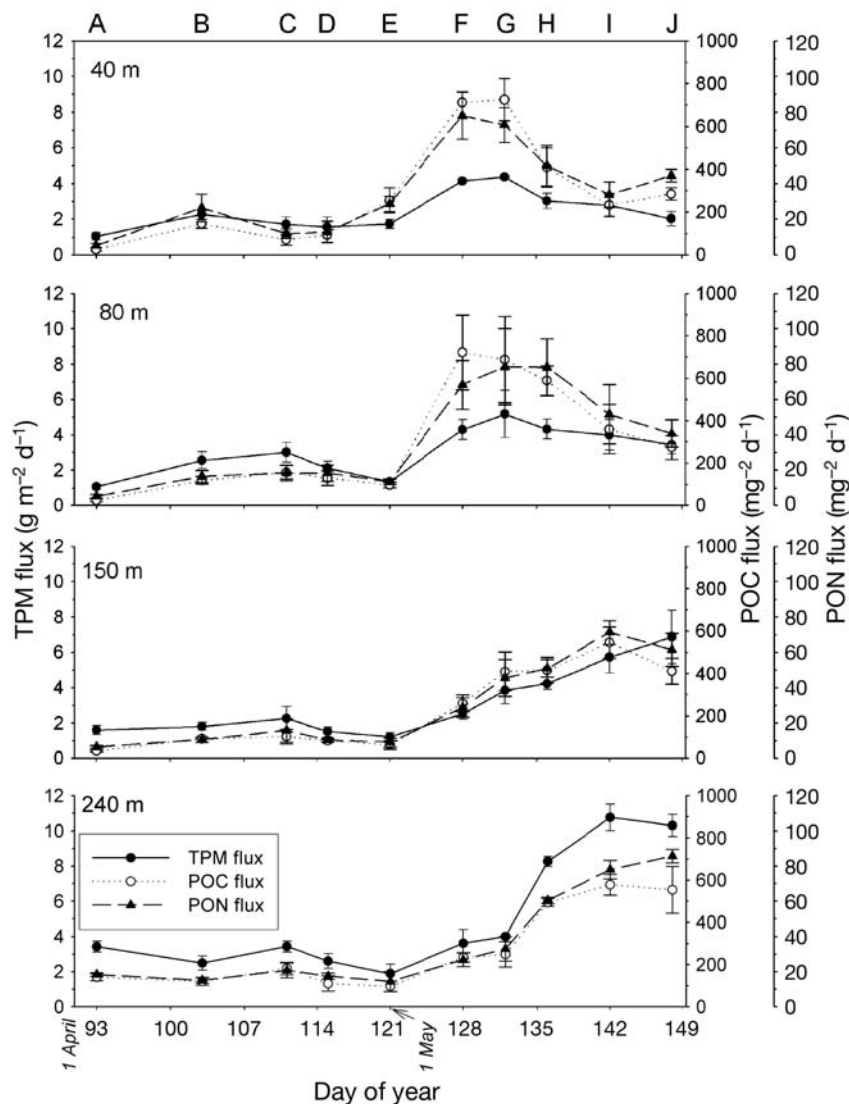


Fig. 3. Mean vertical flux ( $\pm 1$  SD of 4 replicates at each depth) of total particulate matter (TPM, dry weight), particulate organic carbon (POC), and particulate organic nitrogen (PON) vs. day of the year in traps at 40, 80, 150, and 240 m depth. A to J are explained in the legend for Table 1

(Fig. 2c), resulting in significantly greater TPM flux at 80 m than at 40 m (Table 2, Fig. 3). At 150 m, there was a 7-fold increase in TPM flux at the end of May (samples F to J), with an increasing trend to the end of the time series (Fig. 3). A gradual doubling of the organic content occurred from ca. 15% in early April to ca. 30% in early May. At 240 m, a rapid increase in TPM flux was observed in mid-May (sample H), increasing to ca.  $11 \text{ g m}^{-2} \text{ d}^{-1}$  in the third week of May (samples I and J; Fig. 3). TPM flux at 240 m was always significantly higher than at 150 m (Table 2), due in part to resuspension. *In situ* transmissometer readings showed high levels of suspended particles at depths below 200 m, indicating that resuspension periodically reached the level of the 240 m

trap, located 30 m above bottom (mab), but not the 150 m trap at 120 mab. The organic content of the TPM in the 240 m trap reached a maximum of ca. 23% in sample F in early May. At all depths, both mean TPM flux and mean organic content were significantly higher during the sinking event than before it (Table 2), indicating that sedimentation of organic material and not resuspension was responsible for much of the increase in TPM flux at 240 m (Fig. 3). However, there was a significant decrease in percent organic content with increasing trap depth during the sinking event, which was not observed during the pre-event period (Table 2).

Daily fluxes of POC at depths of 40, 80, and 150 m were  $< 35 \text{ mg m}^{-2} \text{ d}^{-1}$  during the first trap deployment (sample A), suggesting little flux of bloom material prior to April (Fig. 3). POC flux increased during April but remained  $< 220 \text{ mg m}^{-2} \text{ d}^{-1}$  at all trap depths until early May. The sinking event was marked by a sudden increase in POC flux during the first week of May at all 4 trap depths (sample F), peaking at  $> 700 \text{ mg C m}^{-2} \text{ d}^{-1}$  at 40 and 80 m (Fig. 3). During mid-May (samples G to I) POC flux to these depths decreased, reaching 200 to  $300 \text{ mg m}^{-2} \text{ d}^{-1}$  by the end of May. POC fluxes  $> 400 \text{ mg C m}^{-2} \text{ d}^{-1}$  were maintained at 150 and 240 m from mid- to late May (samples H to J), with peak values during the third week in May ( $550\text{--}600 \text{ mg m}^{-2} \text{ d}^{-1}$ ; sample I). POC fluxes to 240 m were frequently higher than those to 150 m, presumably due to POC inputs from resuspended bottom

sediments and/or to other sources such as zooplankton fecal pellets released below 150 m. The daily flux of PON followed a similar time course to that of POC (Fig. 3). PON flux increased from  $< 15 \text{ mg m}^{-2} \text{ d}^{-1}$  at all trap depths in April to  $> 70 \text{ mg m}^{-2} \text{ d}^{-1}$  at 40 and 80 m in early May (samples F and G; Fig. 3). PON flux at 150 and 240 m also increased in early May, but reached a maximum later than in the surface traps, with fluxes of  $60\text{--}90 \text{ mg m}^{-2} \text{ d}^{-1}$  in samples I and J. Although the mean fluxes of POC and PON before the sinking event were higher between 150 and 240 m than they were in the upper water column, mean fluxes of POC and PON at all trap depths were equal during the sinking event (Table 2).

Table 2. Mean particle flux (with 95% CL) in Conception Bay, Newfoundland, determined by sediment traps at 4 depths. The sampling period extended from 29 March to 30 May. The number of measurements included in each mean (i.e. sample 'n') ranged from 16 to 24 depending on the variable and depth. 'Pre' refers to the time series before the main sinking event, while 'Event' refers to the main sinking event. 'Pre' and 'Event' were inferred from Figs. 3 & 4. Within each column, mean values sharing the same superscripts are not significantly different ( $p > 0.05$ ; ANOVA followed by post hoc Hochberg GT-2 or Dunnett's T-3 test). Within depths, mean values before and during the main sinking event were significantly different for each constituent ( $p < 0.05$ ). TPM: total particulate dry matter; % org: organic matter as a percentage of total particulate dry matter determined by weight loss on ignition; POC: particulate organic carbon; PON: particulate organic nitrogen

Depth (m)	TPM ( $\text{g m}^{-2} \text{d}^{-1}$ )		% org		POC ( $\text{mg C m}^{-2} \text{d}^{-1}$ )		PON ( $\text{mg N m}^{-2} \text{d}^{-1}$ )	
	Pre	Event	Pre	Event	Pre	Event	Pre	Event
40	1.65 <sup>a</sup> (1.44–1.87)	3.26 <sup>a</sup> (2.84–3.69)	21.7 <sup>a</sup> (19.0–24.3)	40.7 <sup>a</sup> (37.9–43.4)	73.9 <sup>a</sup> (47.0–101)	404 <sup>a</sup> (313–495)	12.3 <sup>a,b</sup> (7.68–17.0)	51.2 <sup>a</sup> (43.0–59.4)
80	2.01 <sup>a</sup> (1.66–2.37)	4.24 <sup>b</sup> (3.83–4.65)	21.4 <sup>a,b</sup> (17.9–24.8)	35.1 <sup>b</sup> (32.9–37.3)	104 <sup>a,b</sup> (79.2–128)	516 <sup>a</sup> (418–614)	14.1 <sup>a,b</sup> (11.3–16.9)	63.5 <sup>a</sup> (54.3–72.6)
150	1.68 <sup>a</sup> (1.46–1.89)	4.63 <sup>b</sup> (3.87–5.39)	19.3 <sup>a,b</sup> (18.3–20.3)	27.2 <sup>c</sup> (25.5–28.9)	72.4 <sup>a</sup> (58.3–86.5)	408 <sup>a</sup> (359–457)	10.1 <sup>a</sup> (8.1–12.0)	50.5 <sup>a</sup> (42.9–58.1)
240	2.77 <sup>b</sup> (2.46–3.08)	7.57 <sup>c</sup> (6.15–8.98)	16.9 <sup>b</sup> (15.0–18.8)	20.2 <sup>d</sup> (19.2–21.1)	130 <sup>b</sup> (113–148)	422 <sup>a</sup> (347–497)	17.3 <sup>b</sup> (14.1–18.8)	53.3 <sup>a</sup> (41.8–65.0)

### Pigment flux

Silicate and nitrate levels in the UML at the time sampling began were lower than in deeper water, indicating that the spring phytoplankton bloom had begun earlier (Fig. 2d,e). However, the first trap sample (A) was clearly taken before any sinking of spring phytoplankton had taken place (Fig. 4). Daily fluxes of total chloropigments (Tchl, i.e. chl *a* + phaeopigments, determined from fluorometric analysis before acidification of the sample) were  $< 0.5 \text{ mg m}^{-2} \text{d}^{-1}$  during the first trap deployment in late March (sample A). During the next 18 d, fluxes of Tchl increased 3- to 4-fold at all trap depths (samples B and C), followed by further increases after the storm, beginning at the end of April at 40 m (sample E) and in early May at all other depths (sample F; Fig. 4). Peak fluxes  $> 10 \text{ mg Tchl m}^{-2} \text{d}^{-1}$  occurred at depths of 40 and 80 m during early to mid-May, with the highest values often observed at 80 m. In late May, Tchl flux decreased to about  $5 \text{ mg m}^{-2} \text{d}^{-1}$  at 40 and 80 m. The accumulation rates of Tchl in traps at 150 m were similar to those at 240 m, with maxima of ca.  $8 \text{ mg m}^{-2} \text{d}^{-1}$  (Fig. 4). There was a time lag as the Tchl flux maximum reached each depth, with maxima occurring in sample F at 40 m, sample G at 80 m, samples G and H at 150 m, and sample H at 240 m (Fig. 4). The mean flux of Tchl was not statistically different among the trap depths before the sinking event, whereas during the event Tchl flux at 80 m was significantly greater than at 240 m (Table 3).

The composition of the chloropigment pool varied seasonally and with depth (Fig. 4). Phaeopigments made a larger contribution to Tchl than did chl *a* at all depths during the first 3 wk of April. Chl *a* flux began to increase in late April at 40 m depth (sample E) and in early May in deeper water (sample F). Values of  $> 8 \text{ mg m}^{-2} \text{d}^{-1}$  were recorded at 40 and 80 m in May, exceeding phaeopigment flux for the entire month at these depths (Fig. 4). Chl *a* flux reached  $2\text{--}4 \text{ mg m}^{-2} \text{d}^{-1}$  at 150 and 240 m (samples F to H), exceeding phaeopigment flux only in sample G at 150 m. During the middle of May, chl *a* decreased with increasing depth from a maximum of 80% of Tchl at 40 m to 30–40% at 240 m. The mean flux of both chl *a* and phaeopigments was significantly greater at all trap depths during the sinking event than before it (Table 3). However, the mean flux of phaeopigments below 40 m did not vary with depth either before or during the sinking event,

Table 3. Mean pigment flux ( $\text{mg m}^{-2} \text{d}^{-1}$ , with 95% CL) in Conception Bay, Newfoundland, determined by sediment traps at 4 depths. For details see legend for Table 2. At 80, 150 and 240 m depths, the phaeopigment pool was dominated by pyropheophorbide *a*, an indicator of copepod grazing of phytoplankton (Redden 1994). Phaeophorbide *a* and phaeophytin *a* made little contribution to the vertical flux of phaeopigments. Tchl: total chloropigments; Chl *a*: chlorophyll *a*; Phaeo: phaeopigments

Depth (m)	Tchl		Chl <i>a</i>		Phaeo	
	Pre	Event	Pre	Event	Pre	Event
40	1.28 <sup>a</sup> (0.95–1.61)	7.06 <sup>a,b</sup> (6.17–7.94)	0.35 <sup>a</sup> (0.25–0.45)	5.07 <sup>a</sup> (4.39–5.76)	0.93 <sup>a</sup> (0.68–1.17)	2.15 <sup>a</sup> (1.93–2.38)
80	2.04 <sup>a</sup> (1.60–2.48)	9.09 <sup>a</sup> (7.24–10.9)	0.70 <sup>b</sup> (0.51–0.90)	5.63 <sup>a</sup> (4.16–7.10)	1.34 <sup>a</sup> (1.06–1.62)	3.46 <sup>b</sup> (3.04–3.88)
150	1.32 <sup>a</sup> (1.01–1.63)	6.40 <sup>a,b</sup> (5.77–7.05)	0.28 <sup>a</sup> (0.20–0.35)	3.00 <sup>b</sup> (2.53–3.46)	1.04 <sup>a</sup> (0.80–1.28)	3.42 <sup>b</sup> (3.11–3.73)
240	1.47 <sup>a</sup> (1.22–1.73)	6.09 <sup>b</sup> (5.23–6.95)	0.31 <sup>a</sup> (0.25–0.37)	2.16 <sup>c</sup> (1.81–2.51)	1.17 <sup>a</sup> (0.96–1.37)	3.93 <sup>b</sup> (3.35–4.51)



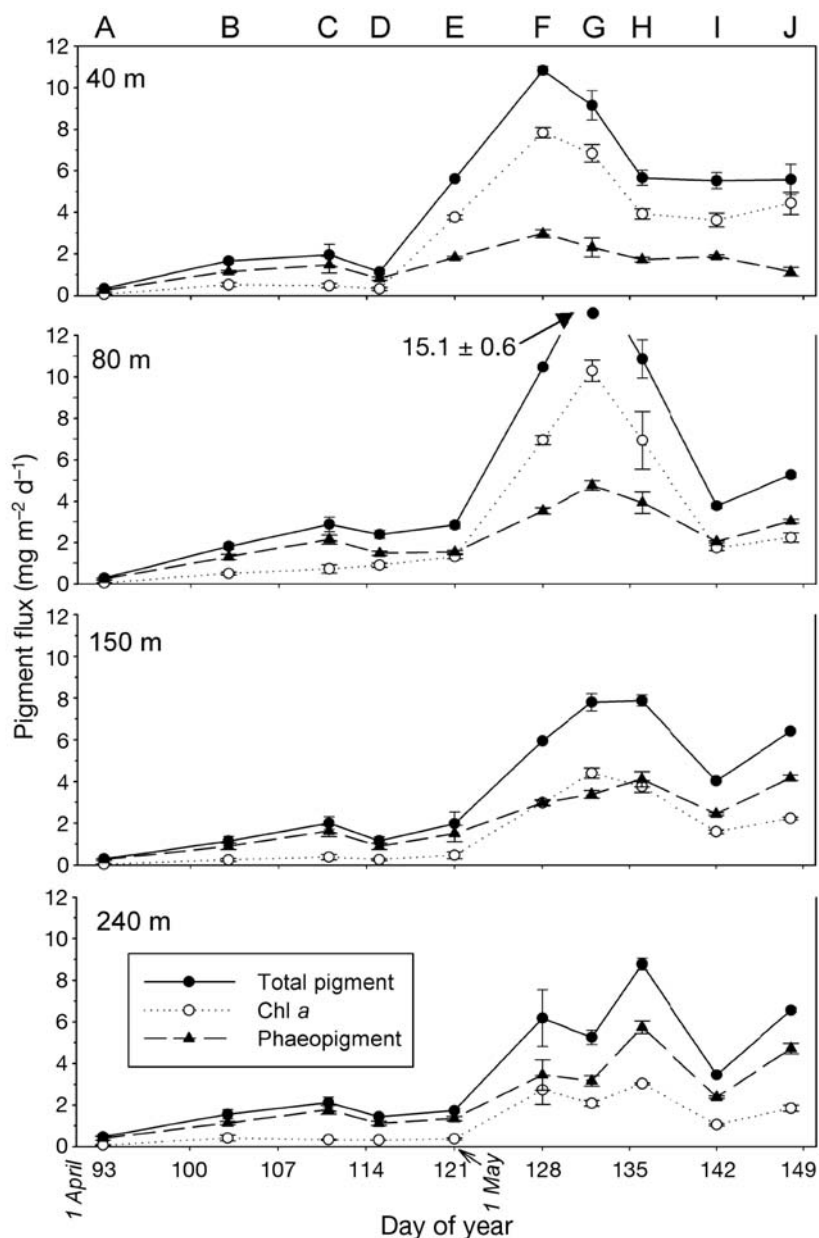


Fig. 4. Mean vertical flux ( $\pm 1$  SD,  $n = 4$ ) of total pigments (total chlorophylls + total phaeopigments), chl *a*, and total phaeopigments (primarily pyropheophorbide and phaeophytin *a*) vs. day of the year in traps at 40, 80, 150, and 240 m depth. A to J are explained in the legend for Table 1

while the mean flux of chl *a* was maximal at 80 m, decreasing at 150 and 240 m both before and during the sinking event (Table 3). The decrease in mean chl *a* flux was greatest between 80 and 150 m, ranging from 60% before the sinking event to ca. 47% during sinking. Pyropheophorbide *a* + other phaeopigments made up about 60% of Tchl in surface sediments from 1 March to 12 September (Redden 1994), similar to material from 240 m traps during the sinking event (i.e. phaeopigments = 65% of Tchl, Table 3).

### Flux quality

C:N ratios for trap material (w/w) were  $\leq 12$  throughout April and May, with maximum values at 40 and 80 m during the first week of May (sample F). Apart from the early phase of the bloom, there was no change in C:N ratio with trap depth (Table 4). Throughout the bloom period, the C:N ratio of particulate material in traps at 240 m fell within a narrow range (6.3 to 8.8). C:N ratios were  $\leq 5.7$  (w/w, i.e. the Redfield ratio) in the 40 and 80 m traps early in April and late in May. C:N ratios at 150 and 240 m varied little during the 8 wk study. Before the sinking event, the mean C:N ratio of trap material at 40 m depth was essentially Redfield, but increased to constant, non-Redfield values of 6.9 to 7.7 at greater depths (Table 4). During the sinking event, the mean C:N ratio at 40 m increased significantly to 9.0, indicating nitrate limitation of phytoplankton (Table 4). The mean C:N ratio did not increase with depth during the sinking event, ranging from 8.0 to 8.1 below 40 m (Table 4).

The sedimentation patterns of pigments reflected those of POC, with little variability in the POC:Tchl ratio during sinking (Table 4). This ratio decreased gradually at all depths during April as pigment flux began to increase. The lowest ratios were recorded in traps below 40 m during late April and early May, when chl *a* flux was high as a result of cell senescence and massive diatom sinking (samples F to H, Fig. 4). The mean POC:Tchl ratio was independent of depth both before and after the sinking event, ranging from 58 to 123 (Table 4). Mean POC:chl *a* was significantly

lower during the sinking event than before, increasing with depth during the sinking event from 82 at 40 m to 233 at 240 m (Table 4). Mean chl *a* content of the sinking material exceeded phaeopigment content only in the 40 and 80 m traps during the sinking event (Table 4). At all other depths and times, phaeopigments made up more than 50% of the sinking material. The importance of zooplankton grazing to phaeopigment flux was suggested by the predominance of pyropheophorbide *a* in the phaeopigment pool.

Table 4. Mean variable ratios (w/w, with 95 % CL) for material from sediment traps at 4 depths in Conception Bay, Newfoundland. For further explanation see legends for Tables 2 and 3

Depth (m)	C:N		POC:Chl a		POC:Tchl		Phaeo:Chl a	
	Pre	Event	Pre	Event	Pre	Event	Pre	Event
40	5.4 <sup>a</sup> (4.8–5.9)	9.0 <sup>a</sup> (8.3–9.8)	294 <sup>a</sup> (231–358)	82 <sup>a</sup> (72–93)	71 <sup>a</sup> (56–87)	59 <sup>a</sup> (52–67)	3.0 <sup>a,b</sup> (2.5–3.6)	0.4 <sup>a</sup> (0.4–0.4)
80	6.9 <sup>b</sup> (6.2–7.6)	8.0 <sup>a</sup> (7.4–8.6)	299 <sup>a</sup> (184–414)	111 <sup>a,b</sup> (87–134)	64 <sup>a</sup> (56–72)	58 <sup>a</sup> (48–68)	2.9 <sup>a</sup> (1.9–3.9)	0.8 <sup>b</sup> (0.7–1.0)
150	7.1 <sup>b</sup> (6.4–7.7)	8.1 <sup>a</sup> (7.6–8.6)	442 <sup>a</sup> (265–620)	164 <sup>b,c</sup> (118–210)	69 <sup>a</sup> (54–83)	70 <sup>a</sup> (54–85)	4.7 <sup>b</sup> (3.7–5.7)	1.3 <sup>c</sup> (1.1–1.4)
240	7.7 <sup>b</sup> (7.3–8.2)	8.0 <sup>a</sup> (7.7–8.3)	785 <sup>a</sup> (344–1225)	233 <sup>c</sup> (157–309)	123 <sup>a</sup> (73–174)	76 <sup>a</sup> (54–97)	4.3 <sup>a,b</sup> (3.6–5.0)	1.9 <sup>d</sup> (1.7–2.2)

The contribution of recognizable phytoplankton cells to carbon flux was much greater at 40 and 80 m than in deeper water (data not shown). Phytoplankton flux at 40 and 80 m began to increase during the last week of April (sample E), with the greatest flux at 80 m in sample F. Excepting sample E at 80 m, chains of *Thalassiosira* spp. accounted for more than 70% of phytoplankton biomass in the 40 and 80 m traps at the times of maximum chl a flux (Fig. 5, samples E to G). With the exception of sample G at 240 m, *Thalassiosira* spp. also accounted for more than 80% of the biomass of phytoplankton at 150 and 240 m at these times (samples F and G; Fig. 5). Sample G at 240 m was dominated by the autotrophic flagellate *Chrysochromulina* sp., which was also abundant in 80, 150, and 240 m traps in early April (sample A). Following the sinking of *Thalassiosira* spp. in the first half of May, the chain-forming diatoms *Chaetoceros* spp. were the most prominent of the recognizable cells in the 40, 80, and 150 m traps (samples I and J) in terms of biomass (Fig. 5). This is consistent with water column data, which indicated that *Chaetoceros* spp. did not regain their earlier predominance until late May, well after the storm. By the end of the time series, the sinking *Chaetoceros* cells had not yet reached the 240 m traps, which were still largely composed of *Thalassiosira* spp. Floc layer samples

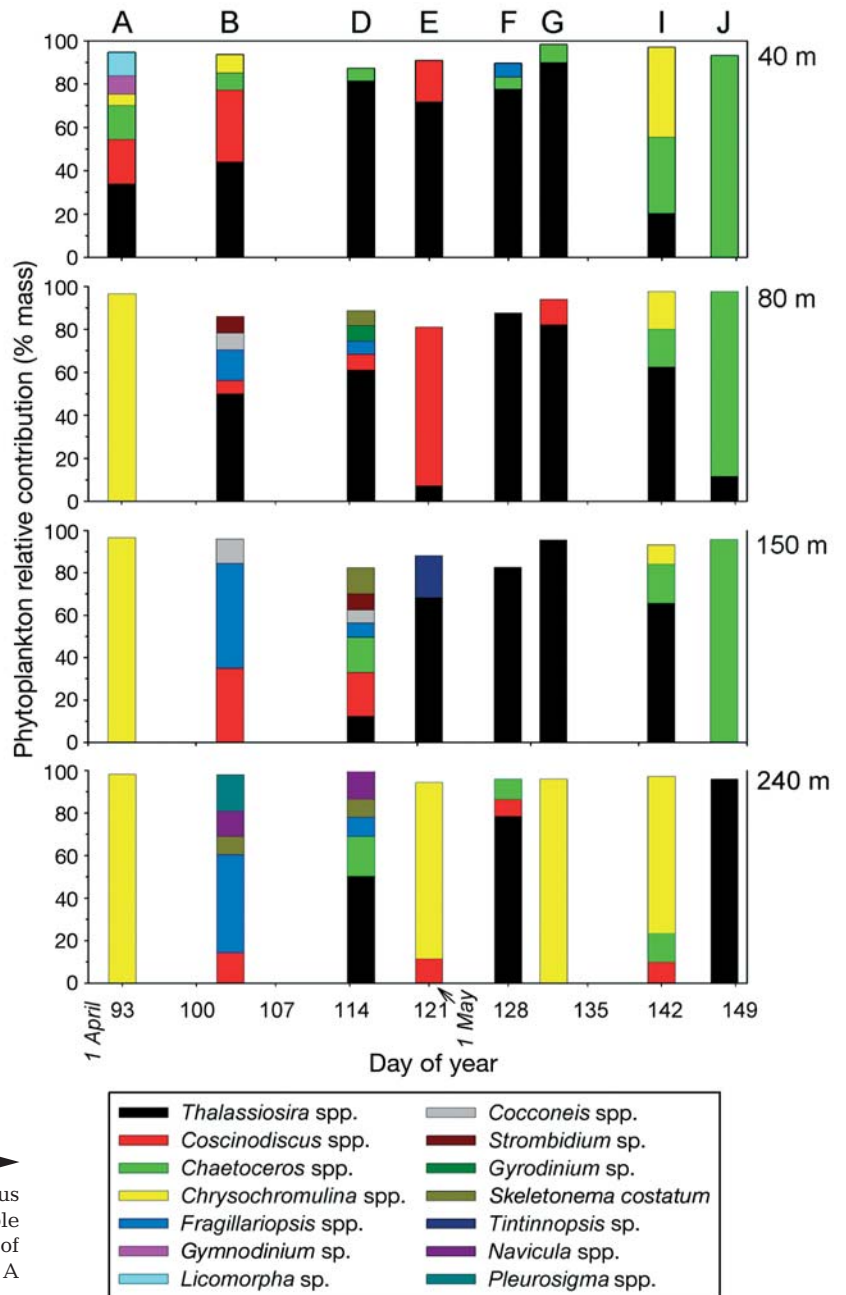


Fig. 5. Relative contribution (by mass) of various phytoplankton species to the total recognizable phytoplankton biomass (by microscopy) vs. day of the year in traps at 40, 80, 150, and 240 m depth. A to J are explained in the legend for Table 1

from the sediment surface were also examined, revealing only a few benthic, pennate diatoms in March, but auxospores of several *Chaetoceros* species were common by the middle of May at volume concentrations similar to those in the UML (i.e.  $3 \times 10^5 \text{ l}^{-1}$ ). After 5 July, there were no recognizable phytoplankton cells in the sediment floc layer.

Fecal pellets made the largest contribution to trap carbon content in mid-April and late May at 150 and 240 m depths (>90%; Fig. 6). The relative contribution of fecal pellet carbon to total recognizable particle mass decreased in early May at all depths, comprising ca. 70% of total carbon content at 150 and 240 m but only 20% at 40 and 80 m. This decrease in fecal pellet contribution to trap contents relative to diatom cells was not simply due to an increase in phytoplankton flux, but rather to a combination of increasing phytoplankton flux and decreasing pellet flux, as the volume concentration of feces decreased 10-fold during the peak of the sinking event at all trap depths. Fecal pellet contents were dominated by resting spores and vegetative cells of *Chaetoceros* spp., as well as other centric diatoms and a few pennate forms.

### Cumulative flux

The temporal trends in carbon flux were similar at all depths, with cumulative flux for the 62 d trap deployment period ranging from  $13.5 \text{ gC m}^{-2}$  at 150 m to  $16.5 \text{ gC m}^{-2}$  at 80 m (Table 5). Presumably cumulative flux was greater at 80 than at 40 m because some of the phytoplankton production occurred below the 40 m trap, and was greater at 240 than at 150 m due to resuspension of organic material and/or defecation by verti-

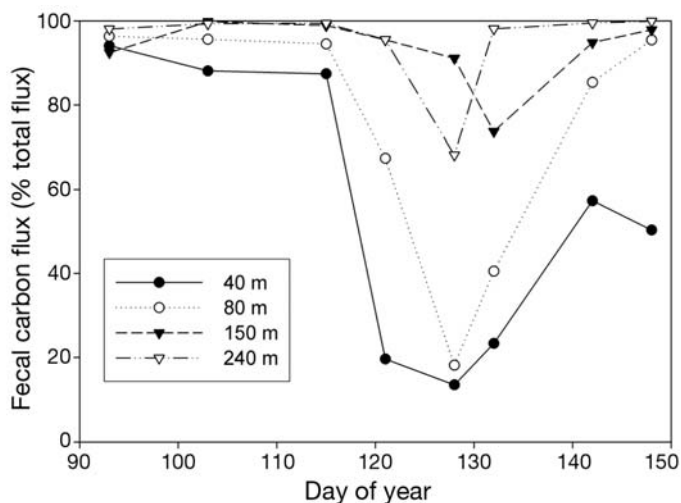


Fig. 6. Zooplankton fecal pellet flux at 40, 80, 150, and 240 m depths vs. day of the year as a relative proportion of total organic carbon flux at each depth

Table 5. Cumulative flux of organic carbon ( $\text{gC m}^{-2}$ ) and total chlorophylls ( $\text{g m}^{-2}$ ) determined by sediment traps from 29 March to 30 May (62 d) in Conception Bay, Newfoundland. For explanation of 'estimated' flux see Results

Trap depth (m)	POC measured	POC (estimated)	Total chlorophylls
40	15.9	—	0.26
80	16.5	—	0.27
150	13.5	20.0	0.20
240	16.0	25.0	0.20

cally migrating zooplankton below 150 m. Cumulative Tchl flux was similar at 40 and 80 m (i.e.  $0.26\text{--}0.27 \text{ g m}^{-2}$ ) and at 150 and 240 m ( $0.20 \text{ g m}^{-2}$ ; Table 5). The trap deployment period did not encompass the entire POC sinking event at 150 and 240 m (Fig. 3). Assuming a similar temporal profile of the sinking event at 150 and 240 m as at 80 m, we estimated the flux of POC over the entire event (ca. 79 d) to be ca.  $20 \text{ gC m}^{-2}$  at 150 m and  $25 \text{ gC m}^{-2}$  at 240 m, about 50% greater than the observed POC fluxes at these depths (Table 5).

## DISCUSSION

### Vertical flux

The spring bloom in Conception Bay begins during mid- to late March in response to increasing light intensity and photoperiod and decreasing wind stress (Stead & Thompson 2003). During initiation of the bloom, the water column is isothermal and  $<0^\circ\text{C}$ . Throughout the course of the bloom, temperatures at and below the SCM are always  $\leq 0^\circ\text{C}$  (our Fig. 2, Parrish et al. 2005). Thus, salinity primarily regulates vertical stability during the bloom period, as is typical of other boreal and sub-arctic coastal environments (Tamelander & Heiskanen 2004). Maximum chl *a* concentrations of ca.  $2.5 \mu\text{g l}^{-1}$  were observed during the first week of May. This relatively low value, probably attributable to a storm in early April, is about half the peak values recorded during spring blooms in Conception Bay in other years (Stead & Thompson 2003).

Although spring phytoplankton production in Conception Bay begins during March, over 75% of the vertical flux of spring POC and phytoplankton pigments from the euphotic zone occurs in May (Stead & Thompson 2003, this study). Vertical flux increases following nutrient depletion and subsequent cell senescence during early May, as indicated by elevated levels of chlorophyllide *a* in sediment traps at 40 to 150 m (Redden 1994). A reduction in the daily POC and pigment flux to 40 and 80 m from mid- to late May signals the decline of

the spring phytoplankton bloom (Figs. 3 & 4). Bloom termination in Conception Bay is also marked by decreasing compound-specific fatty acid  $\delta^{13}\text{C}$  values in the seston (Ostrom et al. 1997), suggesting severe limitation of phytoplankton by dissolved inorganic carbon (Ramos et al. 2003), which decreases by 33 % during the course of the bloom (Ostrom et al. 1997).

The mean and maximum fluxes of TPM, POC, PON, chl *a*, and phaeopigments in Conception Bay are high relative to values from most coastal studies around the world, including upwelling systems. Fluxes in Conception Bay are most similar to data from boreal and subarctic waters, and fall in the middle of the range observed by Colombo et al. (1996) at 150 m in the Gulf of St. Lawrence in May (TPM flux 5–9  $\text{g m}^{-2} \text{d}^{-1}$ ; POC flux 225–275  $\text{mg m}^{-2} \text{d}^{-1}$ ; PON flux 25  $\text{mg m}^{-2} \text{d}^{-1}$ ). POC flux in Conception Bay is also similar to rates for Dabob Bay, Washington, USA (21–470  $\text{mgC m}^{-2} \text{d}^{-1}$  at 60 m, Downs & Lorenzen 1985), the Peru Upwelling at 50 m depth (224–418  $\text{mgC m}^{-2} \text{d}^{-1}$ , Wakeham et al. 1984), the Santa Barbara (California) channel in May following a spring bloom of *Chaetoceros* spp. (Passow et al. 2001), and at 4 stations in the Barents Sea (410–1090  $\text{mgC m}^{-2} \text{d}^{-1}$ ; Andreassen & Wassmann 1998). Peak fluxes of chl *a* are similar in Conception Bay and the Barents Sea (3–10 and 2–13  $\text{mg m}^{-2} \text{d}^{-1}$ , respectively), as are peak fluxes of phaeopigments (4–6 and 3–11  $\text{mg m}^{-2} \text{d}^{-1}$ , respectively, Andreassen & Wassmann, 1998). Maximum POC and chl *a* fluxes in Conception Bay are much lower than those observed by Olesen (1995) at a shallow (30 m) site in the Kattegat (ca. 1400  $\text{mgC m}^{-2} \text{d}^{-1}$  and 1100  $\text{mg chl a m}^{-2} \text{d}^{-1}$ ), but are much greater than off the Antarctic peninsula (ca. 15  $\text{mgC m}^{-2} \text{d}^{-1}$  and 0.23  $\text{mg chl a m}^{-2} \text{d}^{-1}$ , Mincks et al. 2005), in an Antarctic bay (60–120  $\text{mgC m}^{-2} \text{d}^{-1}$ , Baldwin & Smith 2003), and in Storfjorden, Svalbard (ca. 90  $\text{mgC m}^{-2} \text{d}^{-1}$  in September, Glud et al. 1998).

The peak fluxes of POC and Tchl in Conception Bay, ca. 800 and 10  $\text{mg m}^{-2} \text{d}^{-1}$  respectively, occur at 80 m

depth in mid-May. This timing agrees with published data, which suggest that chloropigments begin to arrive at the sediment surface shortly after bloom initiation in late March, with peak flux values generally occurring in late May or June (Stead & Thompson 2003). The peak POC flux at 80 m is about double that measured in Conception Bay by Parrish et al. (2005), while the peak chl *a* flux is about 4-fold higher. During the primary sinking event, we observed a similar pattern of chl *a* and phaeopigment concentration vs. depth as did Andreassen & Wassmann (1998), i.e. chl *a* > phaeopigments above 60 to 80 m depth and phaeopigments > chl *a* at depths >80 m. However, outside the primary sinking event in Conception Bay, phaeopigment concentrations exceeded chl *a* concentrations at all depths.

Estimated cumulative POC flux from the euphotic zone during the development and decline of the spring phytoplankton bloom in Conception Bay is highest at 240 m (25  $\text{gC m}^{-2}$ ) and lowest at 40 m (16  $\text{gC m}^{-2}$ , Table 5). These values are greater than seasonal cumulative sedimentation in the northern Baltic Sea (5.3  $\text{gC m}^{-2}$ , Tamelander & Heiskanen 2004). The POC flux at 240 m is equivalent to 56 % of the estimated primary production of 45  $\text{gC m}^{-2}$  during this 2 mo period (Table 6), and greater than the range of daily fluxes to 100 m in the northeastern Atlantic Ocean (10 to 40 % of primary production, Turley et al. 1995).

Cumulative Tchl flux at 240 m during the sinking event was 0.20  $\text{g m}^{-2}$  (Table 5). Given that 35 % of Tchl is undegraded chl *a* (Table 3), this is equivalent to a cumulative, seasonal flux of chl *a* of 70  $\text{mg m}^{-2}$ . Chl *a* is mixed to at least 10 cm depth in the sediments at the bottom of Conception Bay (Redden 1994), perhaps as a result of the high densities of head-down, deposit-feeding polychaetes (Scheibe 1991), which subduct chl *a* by burrow irrigation and 'hoeing' of surface sediments (Josefson et al. 2002). This bioturbation results in a uniform concentration of chl *a* in the upper 10 cm

Table 6. Seasonal organic carbon budget (79 d period) for the formation and fate of the spring diatom bloom in Conception Bay, Newfoundland. % PP watcol: percentage of the total primary production utilized in the water column; % PP benthos: percentage of the total primary production utilized in the benthos; % benthic flux: percentage of the estimated benthic flux at 240 m utilized in the benthos. For caveats, parameters and parameter values, see 'Materials and methods: First-order seasonal carbon budget'

Process	$\text{gC m}^{-2}$	% PP watcol	% PP benthos	% benthic flux
Primary production	45	—	—	—
Utilization by water column bacteria	2.1	5	—	—
Utilization by water column mesozooplankton	8.3	18	—	—
Estimated benthic flux at 240 m	25	56	—	—
Anaerobic benthic utilization	2	—	4	8
Aerobic benthic utilization	19	—	42	77
Utilization by suprabenthic zooplankton	1	—	2	4
Utilization by macrobenthos	2.8	—	6	11
Net carbon deposition (by difference)	0.2	—	0.4	0.8



of sediments (Scheibe 1991, Redden 1994, Stead & Thompson 2003), with an areal concentration of 200 mg chl *a* m<sup>-2</sup> (Scheibe 1991). Thus, although the sinking spring bloom results in a large export of undegraded chl *a* from the UML to the benthos (i.e. 70 mg m<sup>-2</sup>), this seasonal flux contributes only 35 % to a much larger pool of sedimentary chl *a*. Since it arrives at the bottom during May (ca. 30 d, Fig. 4), this material represents a mass-specific rate of increase of chl *a* in the sediments of ca. 0.01 d<sup>-1</sup>. Independently collected data for sediment chloropigment content (Redden 1994) shows a 44 % increase in the concentration of chl *a* integrated over the upper 10 cm between April and May, fairly close to the 35 % predicted from our flux measurements and the sedimentary chl *a* values of Scheibe (1991).

High remineralization rates of seasonal pulses of POC accompanied by very low turnover rates of sedimenting chl *a* have been reported frequently in the literature, most recently by Josefson et al. (2002) and Mincks et al. (2005). While some authors have attributed low rates of degradation of chl *a* to sub-zero water temperatures (Beaulieu 2002, Mincks et al. 2005), others have found low rates of degradation even at temperatures >7°C, leading to alternative hypotheses, including rapid burial of chl *a* by deposit feeders (Josefson et al. 2002) and the packaging of chl *a* in diatom resting spores (Beaulieu 2002). We hypothesize that, although the benthos of Conception Bay is permanently cold, since chl *a* is well-preserved in warmer sediments (>7°C) elsewhere (Josefson et al. 2002) the low degradation rates of chl *a* in Conception Bay are probably due to factors other than low temperature, such as burial by deposit feeders (Scheibe 1991) or the predominance of diatom resting spores (this study).

### Quality of sinking material

Small, chain-forming centric diatoms, in particular *Skeletonema costatum*, *Chaetoceros* spp., and *Thalassiosira* spp., generally dominate the spring bloom in Conception Bay, indicating that the bloom is inoculated primarily from planktonic rather than benthic sources (McQuoid & Godhe 2003). These taxa are similar to those that dominate the ice-edge spring bloom in the Barents Sea (Andreassen & Wassmann 1998), in the Kattegat (Olesen 1995), and in the latter stages of arctic spring blooms generally (von Quillfeldt 1997). Dominant phytoplankton species in the sediment traps from Conception Bay are representative of these abundant spring bloom taxa, particularly *Thalassiosira* spp. and *Chaetoceros* spp., the latter occurring frequently in spring sediment trap material around the world (Beaulieu 2002). Sinking velocities during the mass

flux of predominantly intact phytoplankton cells and diatom chains in Conception Bay in early May are 20 to 23 m d<sup>-1</sup>, averaged over all trap depths. These values are similar to those of Passow (1991), who recorded a mass flux of *Chaetoceros* spp. of 16 to 32 m d<sup>-1</sup> during the senescent phase of a spring bloom in the Baltic Sea, and of Pilskaln et al. (1998), who observed sinking velocities of 16 to 25 m d<sup>-1</sup> in Monterey Bay, California. The fecal pellet contribution to this flux in Conception Bay is low, similar to some spring blooms at higher latitudes but greater water temperatures (i.e. 5 % of bloom C flux in the Kattegat, Olesen & Lundsgaard 1995), but not to all such blooms (Andreassen & Wassmann 1998). Our data do not enable us to account for the decrease in the absolute flux of zooplankton fecal pellets during the main phytodetritus sinking event, but possible explanations include a decrease in zooplankton abundance, inhibition of zooplankton grazing by phytoplankton alkaloids, and coprophagy by micro- and mesozooplankton. However, we can conclude that sinking of the spring phytoplankton bloom in Conception Bay occurs at rates commonly observed for nutrient-depleted diatoms. This conclusion is supported by microscopic examination of trap contents (Fig. 5) and by fatty acid analyses, which show the dominant fatty acid in sediment trap samples to be 16:1 $\omega$ 7, typical of diatoms (Parrish et al. 2005). According to chloropigment profiles, relatively undegraded phytoplankton cells and chains account for 54 % of Tchl flux to 80 m, 40 % to 150 m, and 33 % to 240 m. This means that 61 % of the undegraded chl *a* that passes 80 m reaches 240 m, which is comparable to the ratio of 67 % for material passing from 80 to 220 m recorded by Parrish et al. (2005), also in Conception Bay, and compares with a transfer efficiency of ca. 50 % for total lipids, neutral lipids, and polyunsaturated fatty acids (PUFAs; Parrish et al. 2005). The mean phaeopigment:chl *a* ratio was <1.9 at all depths during the sinking event (Table 4), defining the sinking material as 'fresh phytodetritus' (Beaulieu 2002). Furthermore, the mean C:N ratios were relatively low (8–9) and independent of depth during the sinking event in May, in agreement with values from many other sites in the world (C:N = 7–9; Beaulieu 2002).

The patterns of POM, POC, PON, and Tchl flux were similar with both depth and duration of the bloom. POM was high during the bloom and represented 25 to 35 % of TPM. These values are similar to those found in polls in western Norway, but much higher than those reported for Norwegian fjords (Wassmann 1991). Mean POC ranged from 8.8 to 12 % of TPM at and above 150 m, to 5.6 % at 240 m. This is higher than the organic matter proportions at 150 m depth in the Gulf of St. Lawrence (2.6–6.7 %, Colombo et al. 1996), but much lower than the value of 32 % of TPM recorded in

the central North Pacific Ocean at 378 m by Wakeham et al. (1984). Thus preservation of organic material during sinking seems to be greater in Conception Bay than at other coastal sites in the region but not as high as at some other sites globally.

Spring bloom phytoplankton in Conception Bay is rich in neutral (i.e. storage) lipids, particularly during the nutrient limitation phase from mid-bloom onwards, when lipids account for up to 6% of TPM (Parrish et al. 2005). These lipids are rich in PUFAs (40 to 55% of total fatty acids), which are highly conserved during sinking, with PUFA proportions increasing from  $\leq 20\%$  before and immediately after the bloom to 30–35% during maximum bloom deposition at 220 m (Parrish et al. 2005). These PUFA proportions may remain high for 4 to 6 wk during bloom deposition in April and May. The lipolysis and hydrolysis indices were low and did not differ among trap depths, suggesting low levels of utilization of the lipid in the sinking bloom material (Parrish et al. 2005).

#### Fate of spring bloom production

Bloom organic material can be utilized by both water column and benthic heterotrophs. However, in Conception Bay the predominant fate of spring primary production was benthic deposition, estimated to be  $25 \text{ gC m}^{-2}$ , or ca. 56% of the seasonal primary production of  $45 \text{ gC m}^{-2}$  (Table 6). Kudo et al. (2007) recorded the same value ( $25 \text{ gC m}^{-2}$ ) for export to the benthos in another sub-arctic coastal location, Funka Bay, Hokkaido, Japan, although this represented only 38% of spring primary production. Water column heterotrophs utilized  $10.4 \text{ gC m}^{-2}$ , or 23% of total primary production in Conception Bay, with mesozooplankton using over 3 times more carbon than bacteria. Kudo et al. (2007) found that 34% of spring bloom production was decomposed in the deep layer of the water column in Funka Bay. Aerobic utilization by benthic microbes and meiofauna in Conception Bay accounted for ca. 77% of the  $25 \text{ gC m}^{-2}$  reaching the bottom, assuming a linear relationship between aerobic mineralization rate and deposition rate throughout the deposition event (Table 6). This agrees with the relatively high rates of benthic oxygen uptake in Conception Bay relative to temperate and tropical benthos (Glud et al. 1998) and with the rapid remineralization of pulses of organic carbon generally observed in the benthos (days to weeks; Beaulieu 2002), and is consistent with several studies demonstrating that aerobic psychrophilic bacteria in permanently cold ( $-1.7^\circ\text{C}$ ) polar sediments exhibit a high metabolic rate (e.g. Arnosti et al. 1998, Thamdrup & Fleischer 1998, Knoblauch et al. 1999). According to Thamdrup & Fleischer (1998) thermal

adaptation of psychrophiles in such sediments compensates for direct temperature effects on metabolism. In cold sediments receiving relatively high organic input, the microbial community appears to respond to the availability of organic matter rather than to temperature change (Kostka et al. 1999). In the Antarctic, sediment microorganisms are able to exploit pulses of organic material very rapidly, and metabolic transformation of organic matter occurs at rates similar to those observed in temperate regions (Fabiano & Danovaro 1998).

In Conception Bay, utilization of carbon by anaerobic processes, benthopelagic zooplankton, and benthic macrofauna accounted for only ca. 23% of deposited carbon (Table 6). Our first-order budget accounts for over 99% of the estimated benthic flux of  $25 \text{ gC m}^{-2}$  during the sinking event, leaving ca.  $0.2 \text{ gC m}^{-2} \text{ d}^{-1}$  for utilization later or for burial (Table 6). Since the rate of aerobic utilization of the bloom by the benthos is the largest term in the budget, a slight overestimation of this rate could have a large effect on the overall balance. Nevertheless, we conclude that the largest sink for spring bloom particulate primary production in Conception Bay is aerobic utilization by benthic micro- and meiofauna (42% of total primary production), followed by water column mesozooplankton (18%; Table 6).

Of the total primary production during spring, 21% is unaccounted for in our budget (Table 6). Three aspects of water column heterotrophy are poorly constrained. First, we have not estimated microzooplankton grazing. Although microzooplankton abundance was very low at the time of the main sinking event (C. H. McKenzie unpubl. data), some unpublished estimates of microzooplankton grazing in Conception Bay do account for much of the daily primary production during spring (S. Roy pers. comm.). Nevertheless, at present we conclude that microzooplankton grazing is a poorly known component of the carbon budget of Conception Bay. Secondly, the estimate of mesozooplankton biomass during spring, ca.  $0.5 \text{ gC m}^{-2}$  over the upper 50 m in early May (Tian et al. 2003), is an approximation. This value compares with a pre-bloom biomass of  $1.5 \text{ gC m}^{-2}$  in the Greenland Sea, which increases to  $20 \text{ gC m}^{-2}$  during the bloom (Noji et al. 1999), and of ca.  $2 \text{ gC m}^{-2}$  in the Gulf of Maine during the spring bloom (Townsend et al. 1994). The estimate of Tian et al. (2003) was based on daytime tows and was normalized to the upper 50 m. Thus, our estimate did not take into account a potential deep source of mesozooplankton biomass. We would only need to double mesozooplankton biomass to  $1 \text{ gC m}^{-2}$ , closer to the published values mentioned above and within the range reported by Tian et al. (2003) for Conception Bay, to account for the non-utilized carbon in our bud-

get (Table 6). Finally, a growth efficiency of 33% for bacteria was used here to estimate total remineralization (Table 6), but bacterial growth efficiency can vary between 10 and 50% in Conception Bay (Pomeroy et al. 1991). Assuming a value of 10% would have resulted in an estimate of ca.  $6 \text{ gC m}^{-2} \text{ d}^{-1}$  utilized by water column bacteria.

### Is the export exceptional in a global context?

Because water column temperature is  $<0^\circ\text{C}$  during the production and sinking of the spring bloom in Conception Bay, one of our questions was whether the time course, duration, and amplitude of the bloom and its sinking component are exceptional compared with other temperate and boreal seas. Iverson et al. (2000) constructed some empirical regression equations that predict many of the relevant variables in a global context. We compared predictions from these equations to our data and previously published results from a simulation model of Conception Bay (Tian et al. 2003). The Iverson model is empirical, not mechanistic, and is based on relatively few field studies world-wide, mainly in tropical and temperate waters. Thus, our data provide an opportunity to test the applicability of the model to site-specific data from very cold water. In addition, this exercise helps to place our site-specific measurements in a larger, global context and to test predictions that sub-zero temperatures during the spring bloom lead to exceptionally high rates of vertical flux.

Petersen & Curtis (1980) and Pomeroy et al. (1991) hypothesized that benthopelagic coupling is exceptionally efficient in sub-arctic and arctic waters due to suppression of water-column bacterial activity and a lagged response in zooplankton numbers. Based on the annual mean concentration of chl *a* ( $0.41 \pm 0.39 \mu\text{g l}^{-1}$ ; Stead & Thompson 2003), Conception Bay falls into the High Variability (HV) province of Iverson et al. (2000). We therefore used the HV equations of Iverson et al. (2000) to predict annual integrated primary, new, and export production for Conception Bay. Substituting the value of  $0.41 \mu\text{g l}^{-1}$  for annual mean chl *a* concentration into the HV regression equation yields 95% confidence limits (CLs) of 146 to  $156 \text{ gC m}^{-2} \text{ yr}^{-1}$  for primary production. Lacking year round primary production data, we compared this predicted range with the output value from the published model, which is  $129 \text{ gC m}^{-2} \text{ yr}^{-1}$  (Tian et al. 2003). Thus there is no evidence that Conception Bay is exceptionally productive in global terms. Substituting the annual estimate of primary production from Tian et al. (2003) into the Iverson et al. (2000) equation gives a predicted 95% CL range of 41 to  $54 \text{ gC m}^{-2}$  for annual export from the photic

zone to the benthos, very close to the value of  $43 \text{ gC m}^{-2}$  from the model (Tian et al. 2003). Thus the cold environment of Conception Bay does not result in a greater export of organic carbon to the benthos than is typical globally. Assuming that the spring bloom primary production estimate of Redden (1994) of  $45 \text{ gC m}^{-2}$  is all new production, and that primary production during the remainder of the year is largely based on recycled nitrogen, the annual export predicted by the Tian et al. (2003) model of  $43 \text{ gC m}^{-2}$  is essentially equal to the annual new production. Thus, annual exported production and new primary production appear to be in balance in Conception Bay over an annual cycle.

In conclusion, a large proportion of the spring phytoplankton bloom in Conception Bay settles to the benthos as intact cells and chains. Most of the particulate material sedimenting to deep waters and to the benthos does so after nutrient depletion and subsequent cell senescence. This material is of high organic and lipid content, but may be nitrogen-poor due to inorganic nutrient limitation of the bloom. While the sinking flux is high, it is within the predicted 95% CLs of recent global models. Thus, while low temperature may regulate important qualitative properties of the sinking organic material, it does not result in remarkably high flux given the levels of new primary production in Conception Bay.

*Acknowledgements.* We thank M. Riehl and E. Hatfield for technical assistance and Drs. L. R. Pomeroy, W. J. Wiebe, and G. T. Rowe for their energetic collaboration and sharing of data and ideas. This work was made possible by personnel of the Field Services Unit at the Ocean Sciences Centre of Memorial University and was supported by an NSERC Strategic Grant to D.D. and R.J.T. and by NSERC Discovery Grants to R.J.T. and D.D.

### LITERATURE CITED

- Andreassen IJ, Wassmann P (1998) Vertical flux of phytoplankton and particulate biogenic matter in the marginal ice zone of the Barents Sea in May 1993. *Mar Ecol Prog Ser* 170:1–14
- Arnosti C, Jørgensen BB, Sagemann J, Thamdrup B (1998) Temperature dependence of microbial degradation of organic matter in marine sediments: polysaccharide hydrolysis, oxygen consumption, and sulfate reduction. *Mar Ecol Prog Ser* 165:59–70
- Baker ET, Milburn HB, Tennat DA (1988) Field assessment of sediment trap efficiency under varying flow conditions. *J Mar Res* 46:573–592
- Baldwin RJ, Smith KL (2003) Temporal dynamics of particulate matter fluxes and sediment community response in Port Foster, Deception Island, Antarctica. *Deep-Sea Res II* 50:1707–1725
- Bathmann UU, Noji TT, Peinert R (1987) Copepod fecal pellets: abundance, sedimentation and content at a permanent station in the Norwegian Sea in May/June 1986. *Mar Ecol Prog Ser* 38:45–51

- Beaulieu S (2002) Accumulation and fate of phytodetritus on the sea floor. *Oceanogr Mar Biol Annu Rev* 40:171–232
- Bloesch J, Burns NM (1980) A critical review of sediment trap technique. *Schweiz Z Hydrol* 42:15–55
- Booth BC (1993) Estimating cell concentration and biomass of autotrophic plankton. In: Kemp PF, Sherr BF, Sherr EB, Cole JJ (eds) *Handbook of methods in aquatic microbial ecology*, Lewis Publishers, Boca Raton, FL, p 199–206
- Budge SM, Parrish CC (2003) Fatty acid determination in cold water marine samples. *Lipids* 38:781–791
- Choe N, Deibel D (2000) Seasonal vertical distribution and population dynamics of the chaetognath *Parasagitta elegans* in the water column and hyperbenthic zone of Conception Bay, Newfoundland. *Mar Biol* 137:847–856
- Colombo JC, Silverberg N, Gearing JN (1996) Biogeochemistry of organic matter in the Laurentian Trough. I. Composition and vertical fluxes of rapidly settling particles. *Mar Chem* 51:277–293
- Dagg MJ, Whitley TE, Iverson RL, Goering JJ (1982) The feeding, respiration, and excretion of zooplankton in the Bering Sea during a spring bloom. *Deep-Sea Res* 29:45–63
- deYoung B, Sanderson B (1995) The circulation and hydrography of Conception Bay, Newfoundland. *Atmos-Ocean* 33:135–162
- Downs JN, Lorenzen CJ (1985) Carbon:pheopigment ratios of zooplankton fecal pellets as an index of herbivorous feeding. *Limnol Oceanogr* 30:1024–1036
- Drazen JC, Baldwin RJ, Smith KL (1998) Sediment community response to a temporally varying food supply at an abyssal station in the NE Pacific. *Deep-Sea Res II* 45:893–913
- Fabiano M, Danovaro R (1998) Enzymatic activity, bacterial distribution, and organic matter composition in sediments of the Ross Sea (Antarctica). *Appl Environ Microbiol* 64:3838–3845
- Fabiano MA, Pusceddu A, Dell'Anno A, Armeni M and others (2001) Fluxes of phytopigments and labile organic matter to the deep ocean in the NE Atlantic Ocean. *Prog Oceanogr* 50: 89–104
- Glud RN, Holby O, Hoffman F, Canfield DE (1998) Benthic mineralization and exchange in Arctic sediments (Svalbard, Norway). *Mar Ecol Prog Ser* 173:237–251
- Grebmeier JM, McRoy CP (1989) Pelagic-benthic coupling on the shelf of the northern Bering and Chukchi Seas. III. Benthic food supply and carbon cycling. *Mar Ecol Prog Ser* 53:79–91
- Hargrave BT, Burns NM (1979) Assessment of sediment trap collection efficiency. *Limnol Oceanogr* 24:1124–1136
- Heiskanen AS, Leppänen JM (1995) Estimation of export production in the coastal Baltic Sea: effect of resuspension and microbial decomposition on sedimentation measurements. *Hydrobiologia* 316:211–224
- Hobson KA, Fisk A, Karnovsky N, Holst M, Gagnon JM, Fortier M (2002) A stable isotope ( $\delta^{13}\text{C}$ ,  $\delta^{15}\text{N}$ ) model for the North Water food web: implications for evaluating trophodynamics and the flow of energy and contaminants. *Deep-Sea Res II* 49:5131–5150
- Iverson RL, Esaias WE, Turpin K (2000) Ocean annual phytoplankton carbon and new production, and annual export production estimated with empirical equations and CZCS data. *Glob Change Biol* 6:57–72
- Josefson AB, Forbes TL, Rosenberg R (2002) Fate of phytodetritus in marine sediments: functional importance of macrofaunal community. *Mar Ecol Prog Ser* 230:71–85
- Juul-Pedersen T, Nielsen TG, Michel C, Møller EF and others (2006) Sedimentation following the spring bloom in Disko Bay, West Greenland, with special emphasis on the role of copepods. *Mar Ecol Prog Ser* 314:239–255
- Knoblauch C, Jørgensen BB, Harder J (1999) Community size and metabolic rates of psychrophilic sulfate-reducing bacteria in Arctic marine sediments. *Appl Environ Microbiol* 65:4230–4233
- Kostka JE, Thamdrup B, Glud RN, Canfield DE (1999) Rates and pathways of carbon oxidation in permanently cold Arctic sediments. *Mar Ecol Prog Ser* 180:7–21
- Kudo I, Yoshimura T, Lee CW, Yanada M, Maita Y (2007) Nutrient regeneration at bottom after a massive spring bloom in a subarctic coastal environment, Funka Bay, Japan. *J Oceanogr* 63:791–801
- McQuoid MR, Godhe A (2003) Influence of benthic vs. pelagic seeding on coastal diatom bloom development. *J Phycol* 39(s1):42
- Mincks SL, Smith CR, DeMaster DJ (2005) Persistence of labile organic matter and microbial biomass in Antarctic shelf sediments: evidence of a sediment 'food bank'. *Mar Ecol Prog Ser* 300:3–19
- Noji TT, Rey F, Miller LA, Børsheim KY, Urban-Rich J (1999) Fate of biogenic carbon in the upper 200 m of the central Greenland Sea. *Deep-Sea Res II* 46:1497–1509
- Olesen M (1995) Comparison of the sedimentation of a diatom spring bloom and of a subsurface chlorophyll maximum. *Mar Biol* 121:541–547
- Olesen M, Lundsgaard C (1995) Seasonal sedimentation of autochthonous material from the euphotic zone of a coastal system. *Estuar Coast Shelf Sci* 41:475–490
- Ostrom NE, Macko SA, Deibel D, Thompson RJ (1997) Seasonal variation in the stable carbon and nitrogen isotope biogeochemistry of a coastal cold ocean environment. *Geochim Cosmochim Acta* 61:2929–2942
- Parrish CC, Thompson RJ, Deibel D (2005) Lipid classes and fatty acids in plankton and settling matter during the spring bloom in a cold ocean coastal environment. *Mar Ecol Prog Ser* 286:57–68
- Parsons TR (1988) Trophodynamic phasing in theoretical, experimental and natural pelagic ecosystems. *J Oceanogr Soc Jpn* 44:94–101
- Passow U (1991) Species-specific sedimentation and sinking velocities of diatoms. *Mar Biol* 108:449–455
- Passow U, Shipe RF, Murray A, Pak DK, Brzezinski MA, Alldredge AL (2001) The origin of transparent exopolymer particles (TEP) and their role in the sedimentation of particulate matter. *Cont Shelf Res* 21:327–346
- Peinert R, von Bodungen B, Smetacek VS (1989) Food web structure and loss rate. In: Bernhard S (ed) *Productivity of the ocean: present and past*. Wiley Interscience Publishers, Chichester, p 35–48
- Petersen GH, Curtis MA (1980) Differences in energy flow through major components of subarctic, temperate and tropical marine shelf ecosystems. *Dana* 1:53–64
- Piškahn CH, Lehmann C, Paduan JB, Silver MW (1998) Spatial and temporal dynamics in marine aggregate abundance, sinking rate and flux: Monterey Bay, central California. *Deep-Sea Res* 45:1803–1837
- Pomeroy LR, Wiebe WJ, Deibel D, Thompson RJ, Rowe GT, Pakulski JD (1991) Bacterial responses to temperature and substrate concentration during the Newfoundland spring bloom. *Mar Ecol Prog Ser* 75:143–159
- Ramos CS, Parrish CC, Quibuyen TAO, Abrajano TA (2003) Molecular and carbon isotopic variations in lipids in rapidly settling particles during a spring phytoplankton bloom. *Org Geochem* 34:195–207
- Redden AM (1994) Grazer-mediated chlorophyll degradation and the vertical flux of spring bloom production in



- Conception Bay, Newfoundland. PhD thesis, Memorial University, St. John's
- Redden AM, Thompson RJ, Deibel D (1993) Effects of short- and long-term freezing on chloropigments in cultured diatoms and bivalve digestive gland and faeces as determined by standard fluorometry and HPLC. *Arch Hydrobiol* 129:67–87
- Richoux NB, Deibel D, Thompson RJ, Parrish CC (2004a) Seasonal changes in the lipids of *Mysis mixta* (Mysidacea) from the hyperbenthos of a cold-ocean environment (Conception Bay, Newfoundland). *Can J Fish Aquat Sci* 61:1940–1953
- Richoux NB, Thompson RJ, Deibel D, Parrish CC (2004b) Seasonal and developmental variation in the lipids of *Acanthostephia malmgreni* (Amphipoda) from the hyperbenthos of a cold-ocean environment (Conception Bay, Newfoundland). *J Mar Biol Assoc UK* 84:1189–1197
- Richoux NB, Deibel D, Thompson RJ (2004c) Population biology of hyperbenthic crustaceans in a cold water environment (Conception Bay, Newfoundland). I. *Mysis mixta* (Mysidacea). *Mar Biol* 144:881–894
- Rysgaard S, Thamdrup B, Riisgaard-Petersen N, Fossing H, Berg P, Christensen PB, Dalsgaard T (1998) Seasonal carbon and nutrient mineralization in a high-Arctic coastal marine sediment, Young Sound, Northeast Greenland. *Mar Ecol Prog Ser* 175:261–276
- Scheibe S (1991) The benthic macrofauna of the deep sublittoral in Conception Bay (Newfoundland, Canada). MSc thesis, Christian Albrechts University, Kiel
- Smetacek VS (1985a) Role of sinking in diatom life-history cycles: ecological, evolutionary and geological significance. *Mar Biol* 84:239–251
- Smetacek VS (1985b) The annual cycle of Kiel Bight plankton: a long-term analysis. *Estuaries* 8:145–157
- Stead RA, Thompson RJ (2003) The effect of the sinking spring diatom bloom on digestive processes of the cold-water protobranch *Yoldia hyperborea*. *Limnol Oceanogr* 48:157–167
- Stead RA, Thompson RJ, Jaramillo JR (2003) Absorption efficiency, ingestion rate, gut passage time and scope for growth in suspension- and deposit-feeding *Yoldia hyperborea*. *Mar Ecol Prog Ser* 252:159–172
- Strathmann R (1967) Estimating the organic carbon content of phytoplankton from cell volume or plasma volume. *Limnol Oceanogr* 12:411–418
- Strickland JDH, Parsons TR (1972) A practical manual of seawater analysis. *Bull Fish Res Board Can* 167
- Tamelander T, Heiskanen AS (2004) Effects of spring bloom phytoplankton dynamics and hydrography on the composition of settling material in the coastal northern Baltic Sea. *J Mar Syst* 52:217–234
- Thamdrup B, Fleischer S (1998) Temperature dependence of oxygen respiration, nitrogen mineralization and nitrification in Arctic sediments. *Aquat Microb Ecol* 15:191–199
- Tian RC, Deibel D, Thompson RJ, Rivkin RB (2003) Modeling of climate forcing on a cold-ocean ecosystem, Conception Bay, Newfoundland. *Mar Ecol Prog Ser* 262:1–17
- Townsend DW, Cammen LM (1988) Potential importance of the timing of spring plankton blooms to benthic-pelagic coupling and recruitment of juvenile demersal fishes. *Biol Oceanogr* 5:215–229
- Townsend DW, Cammen LM, Holligan PM, Campbell DE, Pettigrew NR (1994) Causes and consequences of variability in the timing of spring phytoplankton blooms. *Deep-Sea Res I* 41:747–765
- Turley CM, Lochte K, Lampitt RS (1995) Transformations of biogenic particles during sedimentation in the northeastern Atlantic. *Philos Trans R Soc Lond B Biol Sci* 348:179–189
- von Quillfeldt CH (1997) Distribution of diatoms in the Northeast Water Polynya, Greenland. *J Mar Syst* 10:211–240
- Wakeham SG, Lee C, Farrington JW, Gagosian RB (1984) Biogeochemistry of particulate organic matter in the oceans: results from sediment trap experiments. *Deep-Sea Res* 31:509–528
- Wassmann P (1991) Dynamics of primary production and sedimentation in shallow fjords and pols of western Norway. *Oceanogr Mar Biol Annu Rev* 29:87–154
- Wassmann P, Bauerfeind E, Fortier M, Fukuchi M and others (2004) Particulate organic carbon flux to the Arctic Ocean sea floor. In: Stein R, Macdonald RW (eds) *The organic carbon cycle in the Arctic Ocean*. Springer, Berlin, p 101–138

Editorial responsibility: Otto Kinne,  
Oldendorf/Luhe, Germany

Submitted: June 8, 2006; Accepted: October 15, 2007  
Proofs received from author(s): March 20, 2008